Since January 2020 Elsevier has created a COVID-19 resource centre with free information in English and Mandarin on the novel coronavirus COVID-19. The COVID-19 resource centre is hosted on Elsevier Connect, the company's public news and information website.

International Immunopharmacology 114 (2023) 109478

Contents lists available at ScienceDirect

International Immunopharmacology

journal homepage: www.elsevier.com/locate/intimp

IFIH1/IRF1/STAT1 promotes sepsis associated inflammatory lung injury via activating macrophage M1 polarization

Ailing Wang [a,b], Xueli Kang [a], Jing Wang [a], Shi Zhang [a,c,*]

[a] Department of Pulmonary and Critical Care Medicine, Central Hospital Affiliated to Shandong First Medical University, Jinan, Shandong, China
[b] Department of Ultrasound, Central Hospital Affiliated to Shandong First Medical University, Jinan, Shandong, China
[c] Jiangsu Provincial Key Laboratory of Critical Care Medicine, Department of Critical Care Medicine, Zhongda Hospital, School of Medicine, Southeast University, Nanjing, China

ARTICLE INFO

Keywords:
ARDS
macrophage M1 polarization
IFIH1
IRF1
STAT1

ABSTRACT

Background: A growing body of research has shown that the phenotypic change in macrophages from M0 to M1 is essential for the start of the inflammatory process in septic acute respiratory distress syndrome (ARDS). Potential treatment targets might be identified with more knowledge of the molecular regulation of M1 macrophages in septic ARDS.

Methods: A multi-microarray interrelated analysis of high-throughput experiments from ARDS patients and macrophage polarization was conducted to identify the hub genes associated with macrophage M1 polarization and septic ARDS. Lipopolysaccharide (LPS) and Poly (I:C) were utilized to stimulate bone marrow-derived macrophages (BMDMs) for M1-polarized macrophage model construction. Knock down of the hub genes on BMDMs via shRNAs was used to screen the genes regulating macrophage M1 polarization in vitro. The cecal ligation and puncture (CLP) mouse model was constructed in knockout (KO) mice and wild-type (WT) mice to explore whether the screened genes regulate macrophage M1 polarization in septic ARDS in vivo. ChIP-seq and further experiments on BMDMs were performed to investigate the molecular mechanism.

Results: The bioinformatics analysis of gene expression profiles from a clinical cohort of 26 ARDS patients and macrophage polarization found that the 5 hub genes (IFIH1, IRF1, STAT1, IFIT3, GBP1) may have a synergistic effect on macrophage M1 polarization in septic ARDS. Further in vivo investigations indicated that IFIH1, STAT1 and IRF1 contribute to macrophage M1 polarization. The histological evaluation and immunohistochemistry of the lungs from the $IRF1^{-/-}$ and WT mice indicated that knockout of IRF1 markedly alleviated CLP-induced lung injury and M1-polarized infiltration. Moreover, the molecular mechanism investigations indicated that knockdown of IFIH1 markedly promoted IRF1 translocation into the nucleus. Knockout of IRF1 significantly decreases the expression of STAT1. ChIP-seq and PCR further confirmed that IRF1, as a transcription factor of STAT1, binds to the promoter region of STAT1.

Conclusion: IRF1 was identified as the key molecule that regulates macrophage M1polarization and septic ARDS development in vivo and in vitro. Moreover, as the adaptor in response to infection mimics irritants, IFIH1 promotes IRF1 (transcription factor) translocation into the nucleus to initiate STAT1 transcription.

Abbreviations: ARDS, acute respiratory distress syndrome; LPS, Lipopolysaccharide; BMDMs, bone marrow derived macrophages; KO, knocking out; CLP, cecal ligation perforation; WT, wide-type; ChIP, chromatin immunoprecipitation; seq, sequence; ICU, intensive care unit; FDR, false discovery rate; SD, standard deviation; ANOVA, one-way analysis of variance; IFIH1, IRF1, Interferon-Induced Helicase C Domain-Containing Protein 1; IRF3, Interferon-Induced Helicase C Domain-Containing Protein 3; STAT1, signal transducer and activator of transcription 1; IFIT3, interferon-induced protein with tetratricopeptide repeats 3; GBP1, guanylate binding protein 1; S, supplementary; GEO, Gene Expression Omnibus; WGCNA, Weighted correlation network analysis; MEs, module eigengenes; PPI, Protein-protein interaction; $IRF1^{-/-}$, IRF1 knockout mice; IL-6, Interleukin-6; CCL2, Chemokine ligand 2; IL-1, Interleukin-1; WB, Western blot; GAPDH, glyceraldehyde-3-phosphate dehydrogenase; ELISA, Enzyme-linked immunosorbent assay; RT-PCR, Reverse Transcription-Polymerase Chain Reaction; IFN, Interferon; TF, transcription factor; TLR4, toll like receptor 4; ERK, extracellular regulated protein kinases; NFκB, nuclear factor kappa-B.

* Corresponding author.
E-mail addresses: 1176432054@qq.com (A. Wang), kangxueli1118@163.com (X. Kang), wj891927@126.com (J. Wang), 394873967@qq.com (S. Zhang).

https://doi.org/10.1016/j.intimp.2022.109478
Received 24 September 2022; Received in revised form 12 November 2022; Accepted 16 November 2022
Available online 30 November 2022

1. Background

A common and severe respiratory disease, acute respiratory distress syndrome (ARDS), accounts for 10 % of all intensive care unit (ICU) hospitalizations and has a 40 % mortality rate [1]. The current COVID-19 pandemic has significantly increased the mortality rate of ARDS in comorbid cases, reaching 93 % [2]. A total of 77.5 % of individuals with ARDS also have sepsis or an infection [3]. The onset of ARDS activates immune cells, leading to uncontrolled and persistent sepsis-induced multi-organ dysfunction [4]. A better understanding of the sepsis-induced pathophysiological mechanism that causes ARDS may allow the development of new treatment options [5].

Sepsis-induced inflammatory lung damage begins with the polarization of macrophages to the M1 phenotype [6,7]. The molecular control of macrophage polarization during the development of ARDS remains largely unknown. Our previous studies [8] showed that 5 hub genes (interferon-induced helicase C domain-containing protein 1, IFIH1; interferon-induced helicase C domain-containing protein 1, IRF1; signal transducer and activator of transcription 1,STAT1; interferon-induced protein with tetratricopeptide repeats 3, IFIT3; and guanylate binding protein 1, GBP1) may exert synergistic effects in macrophage M1 polarization and in the progression of sepsis-induced ARDS. Previous studies [9–12] have confirmed that IFIH1 and STAT1 regulate macrophage M1 polarization and sepsis-induced ARDS. However, it remains unknown whether IRF1, GBP1 and IFIT3 are involved in macrophage M1 polarization and sepsis-induced ARDS.

IRF1, a member of the interferon transcription factor family, coordinates with IRF3 to control the transcription of interferon, which act as antiviral agents. Recent studies have demonstrated that IRF1 simultaneously regulates inflammation, but the precise mechanism remains unknown. Moreover, our earlier research verified that IFIH1 controls macrophage M1 polarization and fosters inflammation by regulating the translocation of IRF3 into the nucleus. According to our bioinformatics analysis, IFIH1, IRF1, STAT1, GBP1, and IFIT3 may be involved in a molecular process that cooperatively controls macrophage M1 polarization. However, elucidation of the detailed mechanisms requires further experimental exploration and validation.

To investigate these mechanisms, we utilized shRNA to knock down the expression of IRF1, IFIT3 and GBP1 to evaluate whether these genes are involved in macrophage M1 polarization. Knockout and rescue experiments were conducted for validation both in vivo and in vitro. In addition, molecular experiments were performed to uncover the mechanism linking these hub genes.

2. Methods

2.1. ARDS patients

Sepsis and ARDS were defined according to the Sepsis 3.0 criteria and 2012 Berlin definition [13,14]. Sepsis-induced ARDS was named septic ARDS. The revised Helsinki Declaration was followed when conducting the current study. The Critical Care Centre at Zhongda Hospital's biological specimen bank provided the samples from the individuals who were included. The Institutional Ethics Committee of Zhongda Hospital approved and oversaw the establishment of this specimen bank in 2017. (Registration number: 2017ZDSYLL105). Figure Supplementary (S) 1 displayed the Ethical documents.

As is descript in our previous study, to screen hub genes involved in ARDS and M1-polarized macrophages, we conducted interrelated bioinformatics analysis of mRNA matrix from 26 septic ARDS patients and gene expression profiles of macrophages. The mRNA matrix from septic ARDS patients was built from the biological specimen bank of the Critical Care, Zhongda Hospital. These gene expression profiles of macrophages were screened from the public Gene Expression Omnibus (GEO) database.

Whole blood was drawn from 26 ARDS patients to evaluate all gene expression patterns using the Human mRNA Microarray V4.0 (Arraystar) chip in order to identify potential candidate genes linked to the severity of ARDS. At the time of ICU triage for this trial, critically ill patients admitted via the emergency department were included. If a patient satisfied the requirements for having ARDS within 24 h of enrolling in the trial, they were considered to have the condition. The following conditions qualified as exclusions: any prior history of cancer, immune or hematological disorders, or treatments including chemotherapeutic drugs or steroids within six months of hospitalization. Within 24 h after being admitted to the ICU, whole blood was collected for the isolation of RNA.

Weighted correlation network analysis (WGCNA) was carried out on all gene expression profiles from the 26 ARDS patients to explore potential genes related to the severity of ARDS [15]. Based on co-expression associations, the WGCNA R program was used to categorize all expressed genes in microarrays into different module eigengenes (MEs). The severity of ARDS was then compared with the MEs using Spearman's correlation that had been adjusted for clusters. For further investigation, the genes from modules that had the highest correlation coefficient and the P value < 0.05 with the severity of ARDS were chosen.

2.2. Screen macrophage M1 polarization related genes

We performed a secondary analysis on the GEO public database (GSE46903, human alveolar macrophages from 125 volunteers) to identify significantly differentially expressed genes between M1 macrophages and M0 and M2 macrophages (fold difference > 2; false discovery rate, $FDR < 0.05$), in order to investigate the genes potentially involved in macrophage M1 polarization [16].

We used the edgeR R package to filter for differentially expressed molecules based on RNA sequencing data and the Limma R tool to find genes that were differently expressed based on mRNA microarray data [17,18]. The method for differentially expressed analysis uses moderated t-tests to construct an empirical Bayesian technique to assess changes in gene expression.

2.3. Screen hub genes

A Venn diagram was also drawn to show the overlap between the genes linked to ARDS severity and macrophage M1 in order to find the possible genes shared by both ARDS and these cells.

We used connection degree analysis to perform hub gene analysis to identify the critical genes (number of neighbours). First, we used the STRING website (https://string-db.org/cgi/input.pl) to plot the protein–protein interaction (PPI) network [19]. Second, R was used to determine the overall connection degree of each network node in order to identify the genes with the greatest connectivity degrees. Hub genes were defined as those located above the first connection degree inflection point [20].

2.4. Sepsis induced ARDS model construction

Animal research in the current study were evaluated and authorized by the Jinan Central Hospital's Animal Care and Use Committee. The Ethical approval document was shown in Figure S2. The laboratory animal facility donated C57BL/6 mice (male, 6–8 weeks old) for use in this investigation (Jinan, China).

There were 3 groups, and each group contained 6 mice.

CLP induced septic ARDS: A septic ARDS model was created using the cecal ligation perforation (CLP) method. The mice underwent lower abdomen hair removal, intraperitoneal administration of 50 mg/kg pentobarbital, then cleaning with 75 percent ethanol. An incision is made along the midline of the abdomen to expose the cecum and prevent vascular damage. A 22-gauge needle was used to puncture the cecum, which was then ligated with silk suture 1 cm from its apex. Fecal

material was then squeezed out of the puncture. The abdominal incision was then two-layered, 4–0 silk sutured closed. Finally, to help the mouse recover from anesthesia, its back was gently put on a warm blanket.

CLP-Sham mice: The sham group's cecum was neither ligated or perforated. Finally, to help the mouse recover from anesthesia, its back was gently put on a warm blanket.

2.5. IRF1 $^{-/-}$ mice

The IRF1 knockout (KO) mice (IRF1$^{-/-}$) were purchased from the Gempharmatech Biosciences (China). The primers were used to test the knockout of IRF1.

5′- GTCCTTGACCTAAGCCCCAT −3′ (Forward), 5′-GCCA-GACTCGGGATAAAACTAC G-3′ (Reverse), fragment size of 386 bp;

Purified amplified products underwent DNA sequencing analysis. The mice utilized for breeding and the following investigations were homozygous IRF1$^{-/-}$ animals. From mouse tail tissue, genomic DNA was isolated, and PCR (Polymerase Chain Reaction) was used to pinpoint particular bands. BMDM were obtained from littermate control and IRF1$^{-/-}$ mice, and portion of the BMDM from IRF1$^{-/-}$ mice were transfected with IRF1 over-expressed plasmid for rescue experiment. Western blot were then used to confirm IRF1 expression in macrophages of each group. (For verification findings, see Figure S5).

2.6. Bone marrow isolation and Macrophage culture

Bone marrow-derived macrophages (BMDMs) were generated largely in accordance with other reports. BM cells were taken from the femur and tibia's medullary cavities on an incredibly clean bench. The erythrocytes were lysed using lysing buffer (BD Pharm LyseTM, USA), washed three times in phosphate-buffered saline (PBS), and then cultivated for seven days at 37 °C in a humidified 5 percent CO2 sterile incubator in fresh DMEM with 10 percent FBS and 20 ng/ml M−CSF. F4/80, which is used to identify BMDMs, was found using flow cytometry.

2.7. Cell culture and reagent treatment

The BMDMs were cultured in Dulbecco's modified medium (DMEM; Wisent Biotechnology, Nanjing, China) containing 10 % foetal bovine serum (FBS; Coring, Australia), 100 IU/ml penicillin, and 100 g/ml Poly (I:C) have undergone strong demonstrations showing that they are the activators of RIG-I and IFIH1. Lipopolysaccharide (LPS) has also been demonstrated time and time again to be the traditional activator for M1 macrophage polarization. Inflammatory cell models for ARDS in animals are frequently created using bacterial lipopolysaccharides, which have been solidly established as important pathogenic components of the disease. In the current investigation, Poly(I:C) and LPS were utilized as M1 macrophage polarization stimulators taking these aspects into account. According to our prior research, the concentrations of LPS (500 ng/mL) and Poly(I:C) (50 ng/mL) were determined.

2.8. Overexpression of IRF1

The full-length coding sequence of IRF1 (NM 001164477.1, 2931 bp) was first amplified by PCR. The primer:

Xhol-IRF1-F: ATACTCGAGCGATGCCAATCACTCGAATGCGGATGA.

NotI-IRF1-R: ATAGCGGCCGCTCATCCGCATTCGAGTGATTGGCAT.

The empty vector served as treatment controls. The entire production process was examined in our previous work. The IRF1 over-expression vector and an empty vector were transfected into several BMDMs. Western blots were used to evaluate how over-expression affected the results.

2.9. Knocking down IFIH1/IRF1/STAT1/GBP1/IFIT3

Three different sequences were developed specifically for mouse IFIH1, IRF1, STAT1, GBP1, and IFIT3, according to GeneChem Co., ltd. (https://www.genechem.com.cn; Table S1-S5). BMDMs were transfected using lentivirus supernatant (infection multiplicity = 50). Three days after transfection, we utilized a western blot to evaluate which shRNA was most successful in down-regulating specific genes. The sequences of the most efficient shRNAs are finally shown in bold italics in Table S1–S5. The control sequence was designated as shCtrl and was TTCTCCGAACGTGTGTCACGTT. The knock down effectiveness was evaluated by Western blot, as seen in Figure S4.

2.10. Evaluation of lung histopathology

The right upper lobe was sectioned sagittally into five 5-meter thick sections after being preserved in paraffin. The sections were stained with hematoxylin and eosin. Edema, alveolar and interstitial inflammation and bleeding, atelectasis, necrosis, and the development of the hyaline membrane were all rated on a scale from 0 to 4. The sum of the scores was used to calculate the extent of lung injury, as was previously mentioned. The ratio of lung wet weight to body weight (LWW/BW) in each group was determined to reflect the severity of the pulmonary vascular permeability and pulmonary oedema.

2.11. Flow cytometry

Cultured BMDMs suspension was re-suspended in PBS, incubated for 15 min with FcR blocking reagent, and then incubated for 15 min with an APC-conjugated anti-mouse CD86 (1:200) or FITC-conjugated anti-mouse F4/80 (1:200) antibody, as instructed by the manufacturer, for phenotypic analysis of cell surface marker expression. Macrophages were recognized by the F4/80 macrophage marker, whereas M1 macrophages were recognized by the CD86 M1 macrophage marker. The level of CD86 expression was calculated using fluorescence intensity. The labeled cells were washed twice, resuspended in cold buffer, and then the data were analyzed using flow cytometry (ACEA NovoCyte, China) and FlowJo software version X. (Tree Star, USA).

CD86: Abcam, Mouse anti-Rat mAb #ab218757.

F4/80: Abcam, Mouse anti-Rat mAb #ab60343.

2.12. Immunohistochemical staining

Slices of lung were moistened and deparaffinized. Slides were blocked with 5 percent goat serum for an hour after antigen extraction at a high temperature. The sections were incubated with primary antibodies overnight at 4 °C after blocking (diluted 1:100). The primary antibodies (Abcam, Mouse anti-Rat mAb #ab218757) were directed against CD86. After three PBS rinses, the slices were then subjected to a 1:50 dilution of a biotinylated secondary antibody. Hematoxylin was used to counterstain the reaction products after diaminobenzidine (DAB, China) incubation. The positive areas were quantified using Image J. All of the photographs were taken using a light microscope at a high magnification (400). (Olympus).

2.13. ELISAa

Interleukin-6 (IL-6), chemokine ligand 2 (CCL2), and interleukin-1β (IL-1β) concentrations in macrophage culture supernatant and bronchoalveolar lavage fluid (BALF) were measured were measured by Enzyme-linked immunosorbent assay (ELISA).

IL-6: Mouse IL-6 ELISA Kit (ab222503), Abcam (England).

CCL2: Mouse ELISA Kit (MJE00B), R&D Systems (The United States).

IL-1β: Mouse IL-1 beta ELISA Kit (ab197742), Abcam (England).

2.14. Western blot (WB) analysis

Proteins were separated using sodium dodecyl sulfate–polyacrylamide gel electrophoresis and then transferred to PVDF membranes. The membranes were treated with primary antibodies overnight at 4 °C against IFIH1 (1:1000), iNOS (1:1000), IRF1 (1:1000), STAT1 (1:1000), IFIT3 (1:1000), GBP1 (1:1000), GAPDH (1:1000), and -Tubulin (1:1000). The secondary antibody was applied to the membranes and left on them for an hour at room temperature. To visualize immunoblots, enhanced chemiluminescence was utilized (ECL; Thermo Scientific). To make the expression levels of the entire cell extract normal, the expression levels of -Tubulin were employed.

iNOS: Abcam, rabbit mAb #ab178945.
β-Tubulin: Abcam, rabbit mAb #ab108342.
IRF1: Abcam, rabbit mAb #ab245338.
STAT1: Abcam, rabbit mAb #ab92506.
IFIH1: Cell Signaling Technology, rabbit mAb #5321.
IFIT3: Invitrogen, rabbit pAb # PA5-22230.
GBP1: Abcam, rabbit mAb # ab119236.
GAPDH: Abcam, rabbit mAb # ab181602.

2.15. PCRa

TRIzol was used to extract the total RNA from lung tissue samples or cells. For reverse transcription of RNA, Takara, Japan's Prime ScriptTM Trimester Mix was used. According to the manufacturer's recommendations, Reverse Transcription-Polymerase Chain Reaction (RT-PCR) was carried out using a Step One Plus RT-PCR equipment (Life Technologies, USA) and SYBR Premix Ex TaqTM11 (Takara, Japan).

Reverse transcription of RNA was carried out using Trimester Mix (Takara, Japan). According to the manufacturer's recommendations, RT-PCR was carried out using a Step One Plus RT-PCR equipment (Life Technologies, USA) and SYBR Premix Ex TaqTM11 (Takara, Japan).

The genomic DNA fragments from transgenic mice's tail snips were identified using agarose gel electrophoresis. With the use of the *Eco*RV restriction enzyme and 1.0 percent agarose gel, DNA samples taken from the transgenic and parental lines were broken down. After that, a flask containing 0.20 g of agarose and 20 ml of 1X Tris-acetate-EDTA buffer was cooked in a microwave for 5 min at 100 °C. Thermo Fisher Scientific, Inc.) was then added, and 2 l of ethidium bromide was poured onto a taped plate with casting combs. Then, 2 μl Once separation was accomplished, samples of mouse tail DNA or macrophage DNA were added to the 5X agarose gel and subjected to electrophoresis at 120 mA for 40 min at 25 °C. The Bio-Rad gel imager was used to see the DNA fragments.

2.16. ChIP-seq and ChIP-PCR

ChIP-seq (chromatin immunoprecipitation sequence) was utilized to investigate whether IRF1 binds to promoter region of STAT1, and ChIP-PCR was conducted to validate the results analyzed by CHIP-seq.

By centrifuging BMDMs, crude nuclear pellets were extracted, resuspended in lysis buffer, and incubated on ice for ten minutes. To create chromatin fragments of around 200–400 bp in length, the chromatin was sonicated at 4 °C using a Bioruptor 300 at the maximum setting for fifteen 1-minute cycles of 30 s on and 30 s off. The soluble chromatin was precleared using protein A agarose beads and diluted 1:10 with dilution buffer. Antibodies against IRF1 were incubated overnight at 4 °C with the precleared supernatant.

After washing, 100 mM NaCl was added, and the immunoprecipitated material was allowed to sit at 65 °C for 12 h before being eluted. The enriched genomic DNA was extracted using phenol, chloroform and isoamyl alcohol, followed by ethanol precipitation, after protein and RNA had been removed. ChIP-seq and ChIP-PCR were used to analyze the immunoprecipitated DNA after it had been dissolved in water. The following were the ChIP-PCR primers:

GCAGTGAGTGAGTGAGAG (Forward).
AGTGAGAACGGCAGGATA (Reverse).

2.17. Statistical analysis

In vivo and in vitro experiments in each group used six and three mice, respectively. Data are expressed as the mean and standard deviation (SD) of repeated trials. One-way analysis of variance (ANOVA) was used to compare among groups. The cut-off value for statistical significance was set at $P < 0.05$.

In these multi-group comparisons, the Tukey's style post-hoc pairwise test were utilized to analysis the high-throughput experiments and a false discovery rate (*FDR*)-adjusted $P < 0.05$ was set as the cut-off [18,21]. These high-throughput experiments included ChIP-seq data and differentially expressed analysis on mRNA microarray data of macrophage polarization (GSE46903).

3. Results

3.1. Three hub gene molecules may play a synergistic role in macrophage M1 polarization

The interrelated analysis was performed on high-throughput experimental data from peripheral blood samples of 26 ARDS patients (clinical information shown in Table S6) and in vitro human alveolar macrophages from 125 volunteers (GEO public database, GSE46903). The analysis indicated the involvement of the hub genes STAT1, IFIH1, GBP1, IFIT3, and IRF1 (Figure S3), consistent with the results of our previous studies [8].

Prior research has established that STAT1 and IFIH1 are essential for macrophage M1 polarization and inflammation in the lung [8–13,22–25]. To further verify whether GBP1, IFIT3, and IRF1 influence macrophage M1 polarization, shRNA sequences for each gene were added to create transfected BMDMs with GBP1, IFIT3, and IRF1 knockdown. These cells were then subjected to LPS induction for 24 h. The shRNA sequence was able to silence GBP1, IFIT3, and IRF1in BMDMs, as demonstrated in FigureS4.

In contrast to control treatment (control shRNA transfection), Western blot analysis showed that silencing IRF1 significantly reduced LPS-induced iNOS production in BMDMs ($P < 0.05$, Fig. 1). However, GBP1 and IFIT3 knockdown did not influence LPS-induced iNOS expression in BMDMs compared with controls ($P > 0.05$, Fig. 1). In addition, the vector transfection of shRNAs and controls did not influence iNOS expression.

These results suggest that IFIH1, IRF1 and STAT1 may contribute to macrophage M1 polarization synergistically.

3.2. IRF1 contributes to macrophage M1 polarization

To provide solid proof that IRF1 contributes to macrophage M1 polarization, IRF1 deletion, rescue, and over-expression experiments were conducted. Western blots revealed that LPS-induced iNOS expression in BMDMs from $IRF1^{-/-}$ mice was considerably reduced compared to that in BMDMs from WT mice ($P < 0.05$, Fig. 2A). Flow cytometry revealed that CD86 expression was significantly lower after IRF1 knockout ($P < 0.05$, Fig. 2B). Furthermore, vector transfection had no effect on iNOS or CD86 expression ($P > 0.05$). ELISA further indicated that the inflammatory cytokine levels of IL1β, IL6, and CCL2 were significantly decreased in culture medium after deleting IRF1 ($P < 0.05$, Fig. 2C/D/E).

Rescue experiments showed that BMDMs from the $IRF1^{-/-}$ mice were transfected with IRF1 high expression plasmid, and the expression of iNOS and CD86 increased again after LPS stimulation. In the above rescue experiment, the pro-inflammatory factors IL-1β, IL-6 and CCL2 also showed similar changes (Fig. 2).

Compared with control blank vectors, the M1-polarized markers (iNOS, CD86, L-1β, IL-6 and CCL2) were markedly increased after over-

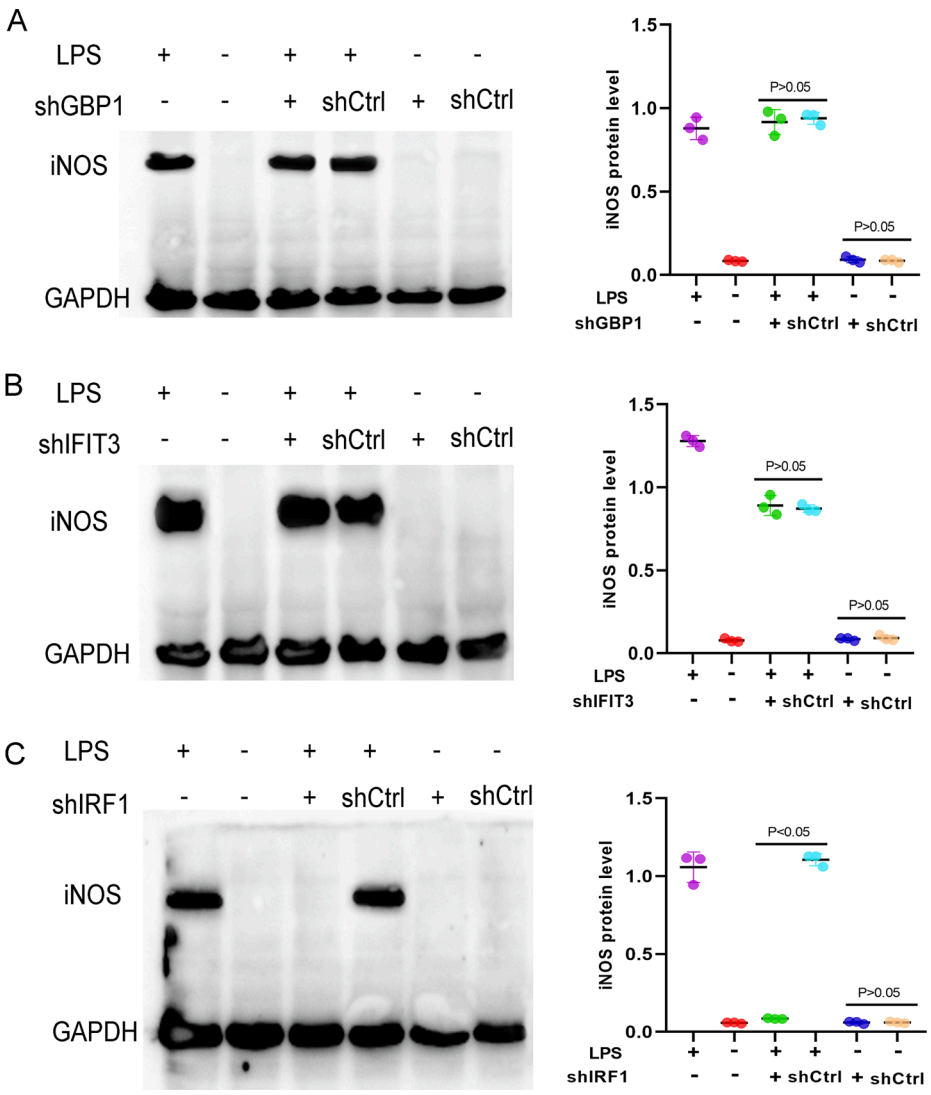

Fig. 1. IFIH1, IRF1 and STAT1 were identified as regulators of macrophage M1 polarization in ARDS. Three mice were included in each group. (A/B/C) In BMDMs, transfected BMDMs with shGBP1, shIFIT3, and shIRF1, as well as control BMDMs with shRNA, the expression of iNOS was detected by Western blotting. After IRF1 silencing, LPS-induced iNOS expression in BMDMs was significantly reduced, according to the quantitative analysis of western blotting ($P < 0.05$). GBP1 and IFIT3 knockdown had no effect on iNOS expression in BMDMs ($P > 0.05$). Additionally, neither the vector transfection of shIFIH1 nor the control shRNA had an impact on the expression of iNOS in BMDMs. The statistical analysis was from three independent experiments, and the bar indicates the SD values.

expression of IRF1in BMDMs from the WT mice ($P < 0.05$, Fig. 2).

These results validated that IRF1 contributes to LPS-induced macrophage M1 polarization.

3.3. IRF1 plays critical roles in ARDS development

We established a CLP-induced septic ARDS model and knocked out the IRF1 gene in mice to further confirm the involvement of IRF1 in the development of ARDS. We next evaluated the effect of IRF1 on lung injury.

We used a histological evaluation of the lungs to confirm the effect of IRF1 on CLP-induced lung injury in mice. Compared with the sham group, acute lung injury caused the CLP model; that is, the pathological specimens showed extensive thickening of the alveolar wall and obvious infiltration of inflammatory cells (Fig. 3A). The lung injury scores in the CLP-IRF1$^{-/-}$ group were significantly lower than those in the CLP-WT group, suggesting that IRF1 could alleviate LPS-induced septic ARDS ($P < 0.01$) (Fig. 3C).

The LWW/BW response to pulmonary oedema is related to the severity of lung injury. In the CLP-induced ARDS mice, the LWW/BW was significantly higher than that in the control group at 24 h ($P < 0.05$) (Fig. 3D). After IRF1 knockout, LWW/BW was significantly reduced in the mice with "CLP-induced ARDS" ($P < 0.05$) (Fig. 3D), suggesting that regulation of low IRF1 expression can effectively inhibit lung injury and alleviate ARDS.

Previous studies have shown that macrophage M1 polarization contributes to particulate matter (PM)-induced lung injury, while inhibition of M1 polarization can alleviate acute lung injury [18]. Therefore, we evaluated the effect of IRF1 knockout on the number of lung macrophages on M1 polarization in ARDS by immunohistochemistry. Compared with the sham group, the proportion of CD86^{+} macrophages in the lungs of CLP-induced ARDS mice was significantly increased (Fig. 3B) ($P < 0.05$), indicating that M1-polarized macrophages aggregated into the lung during pulmonary ARDS. After IRF1 knockout, the proportion of CD86^{+} macrophages in the lungs of the mice were significantly reduced again (Fig. 3B) ($P < 0.05$).

In this study, the levels of IL-1β, IL-6 and CCL2 in the BALF of CLP-induced ARDS mice were significantly higher than those in the BALF of control mice ($P < 0.05$).Knockout of IRF1inhibited the production of the pro-inflammatory cytokines IL-1β, IL-6 and CCL2 (Fig. 3 F-H) in the BALF of mice with CLP-induced ARDS ($P < 0.05$).

These results indicate that high expression of AKDND22 is the critical link in the ARDS inflammatory storm and exacerbation of lung injury.

These results further suggest that IRF1 promotes M1-polarized macrophage lung aggregation in CLP-induced ARDS.

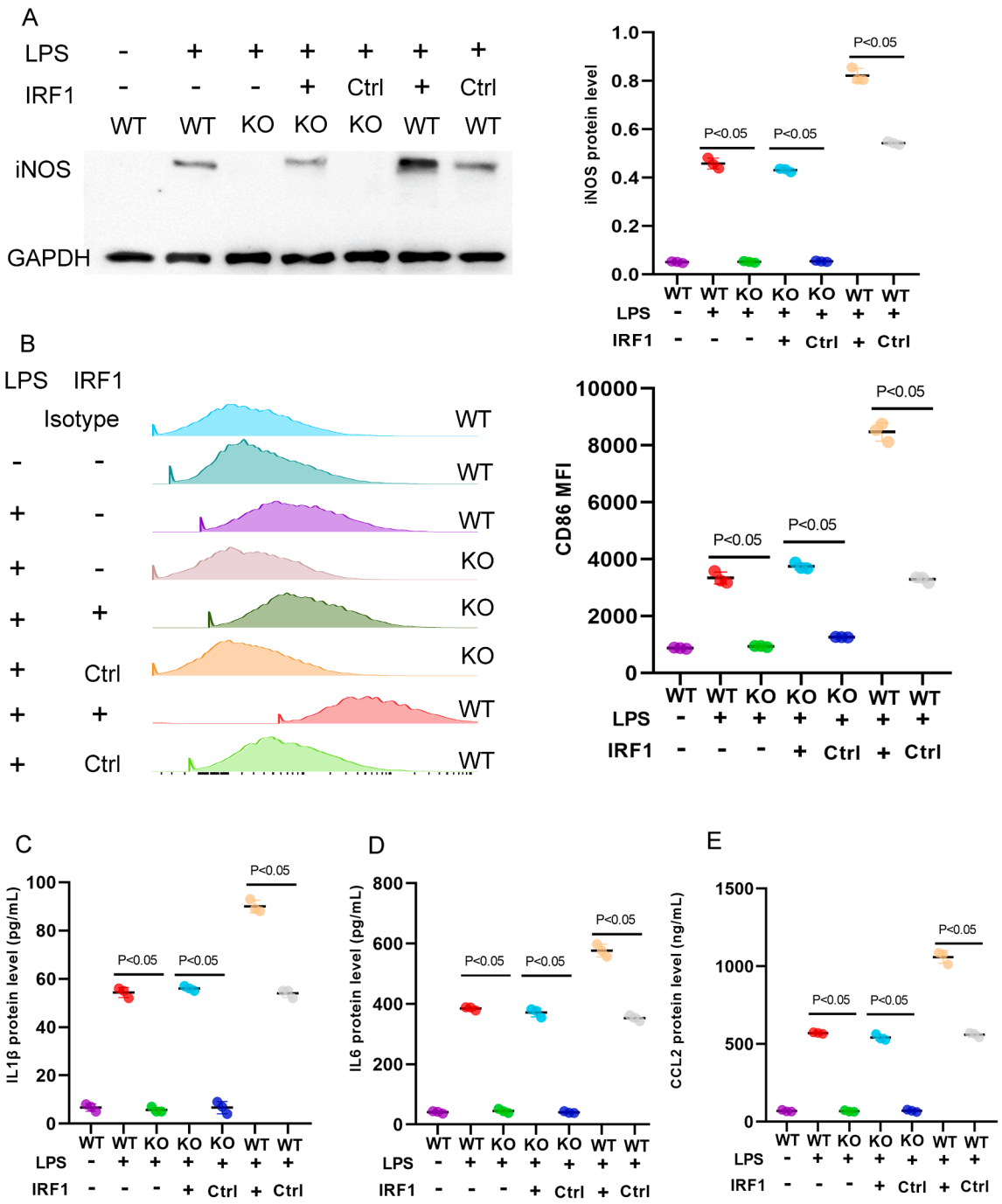

Fig. 2. IRF1 contributes to macrophage M1 polarization. Three mice were included in each group. (A) Western blotting was performed to determine the expression of iNOS on BMDMs with IRF1 knocking out, rescuing and over-expressing. GAPDH was used as the standard for verifying equivalent loading (n = 3 for each group). (B) Flow cytometric analysis was performed to analyze the MFI of CD86 on each group of BMDMs (n = 3 for each group). (C) ELISA detected the expression of IL1β, IL6 and CCL2 in culture medium from each BMDMs (n = 3 for each group). The statistical analysis was from three independent experiments, and the bar indicates the SD values.

3.4. IFIH1 modulates macrophage M1 polarization depending on IRF1 translocation into the nucleus

IFIH1, STAT1 and IRF1 have been validated to be involved in macrophage M1 polarization and septic ARDS in previous studies and the current study. The PPI and WGCNA analyses suggested that these three molecules may synergistically regulate macrophage M1 polarization. To investigate this possibility, we first knocked down IFIH1 expression to evaluate whether IFIH1 could affect IRF1 and STAT1 (transcription factors) translocation into the nucleus.

Western blot analysis of the cell nucleus indicated that IFIH1 knockdown had no effect on STAT1 translocation into the cell nucleus (Fig. 4, $P > 0.05$). Compared with the control treatment (shCtrl), Western blot in the cell nucleus revealed that both Poly (I:C)-induced and LPS-induced expression of IRF1 in BMDM nuclei was significantly reduced after IFIH1 knockdown (Fig. 4, $P < 0.05$). In addition, compared with the control treatment, IFIH1 knockdown had no effect on STAT1 and IRF1 protein expression in BMDMs (Fig. 4, $P < 0.05$).

These results indicate that IFIH1 is an adaptor and signal transduction molecule that activates IRF1 translocation into the nucleus.

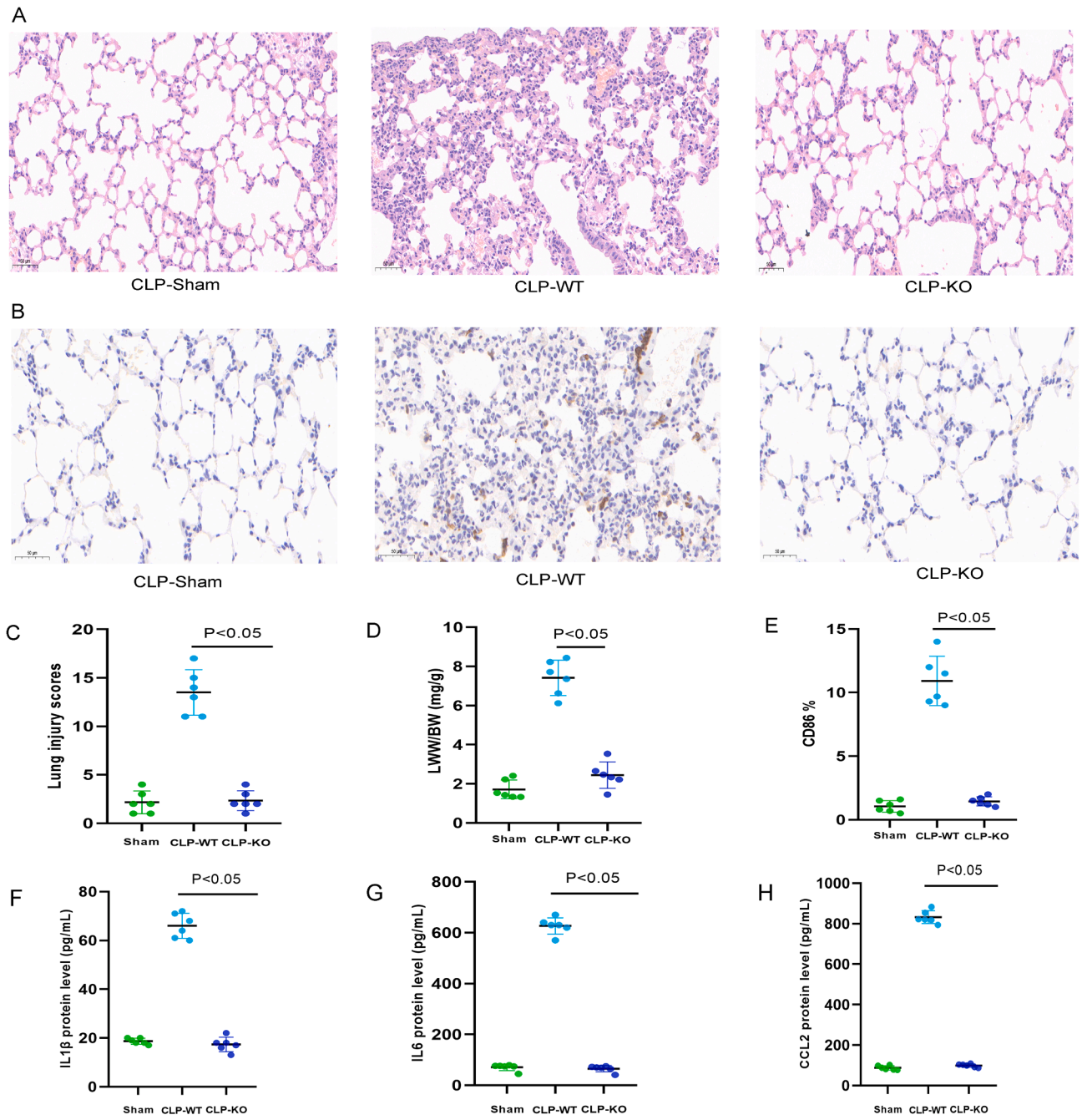

Fig. 3. IRF1 knockout alleviated sepsis induced inflammatory lung injury in mice. There were 3 groups, and each group contained 6 mice. (A) Representative images of lung sections stained with H&E from CLP induced ARDS mice at 24 h, the magnification of microscopic images is × 200 (n = 6 for each group). (B) Representative histopathologic and IHC image of lung tissues from CLP induced ARDS mice at 24 h, the magnification of microscopic images is × 400 (n = 6 for each group). (C) Lung injury scores were estimated by the method of Mikawa (n = 6 for each group). (D) Comparison of the lung wet weight to body weight ratio (LWW/BW) in different groups at 24 h (n = 6 for each group). (E) The percentage of M1-polarized macrophage is assessed through CD86 positive cells to the total cells (n = 6 for each group). (F) Comparison of the pro-inflammatory cytokine IL-1β in alveolar lavage fluid (BALF) by ELISA (n = 6 for each group). (G) Comparison of the pro-inflammatory cytokine IL-6 in BALF by ELISA (n = 6 for each group). (H) Comparison of the pro-inflammatory cytokine CCL2 in BALF by ELISA (n = 6 for each group).

3.5. *IRF1 is the transcription factor of STAT1*

IRF1 and STAT1 are transcription factors that regulate molecular expression. To further explore the molecular mechanism linking IFIH1, STAT1 and IRF1, we knocked down STAT1 expression to assess whether STAT1 influences IFIH1 and IRF1 expression. Then, we utilized BMDMs from IRF1$^{-/-}$mice to evaluate whether IRF1 regulates STAT1 and IFIH1 expression.

Western blotting indicated that STAT1 knockdown did not influence the expression of IRF1 or IFIH1 (Fig. 5A, $P > 0.05$). Western blotting indicated that IRF1 knockout markedly decreased STAT1 expression (Fig. 5B, $P < 0.05$) but did not influence the expression of IFIH1 ($P > 0.05$).

ChIP-seq further found that IRF1 binds to the promoter region of STAT1 (Fig. 5C, *FDR* < 0.05) compared with the input group. The binding region was located on Chr1 start="52118977″ stop="52119911″; the sequence and length are shown in Table S7. ChIP-PCR further confirmed that IRF1 binds to the promoter region of

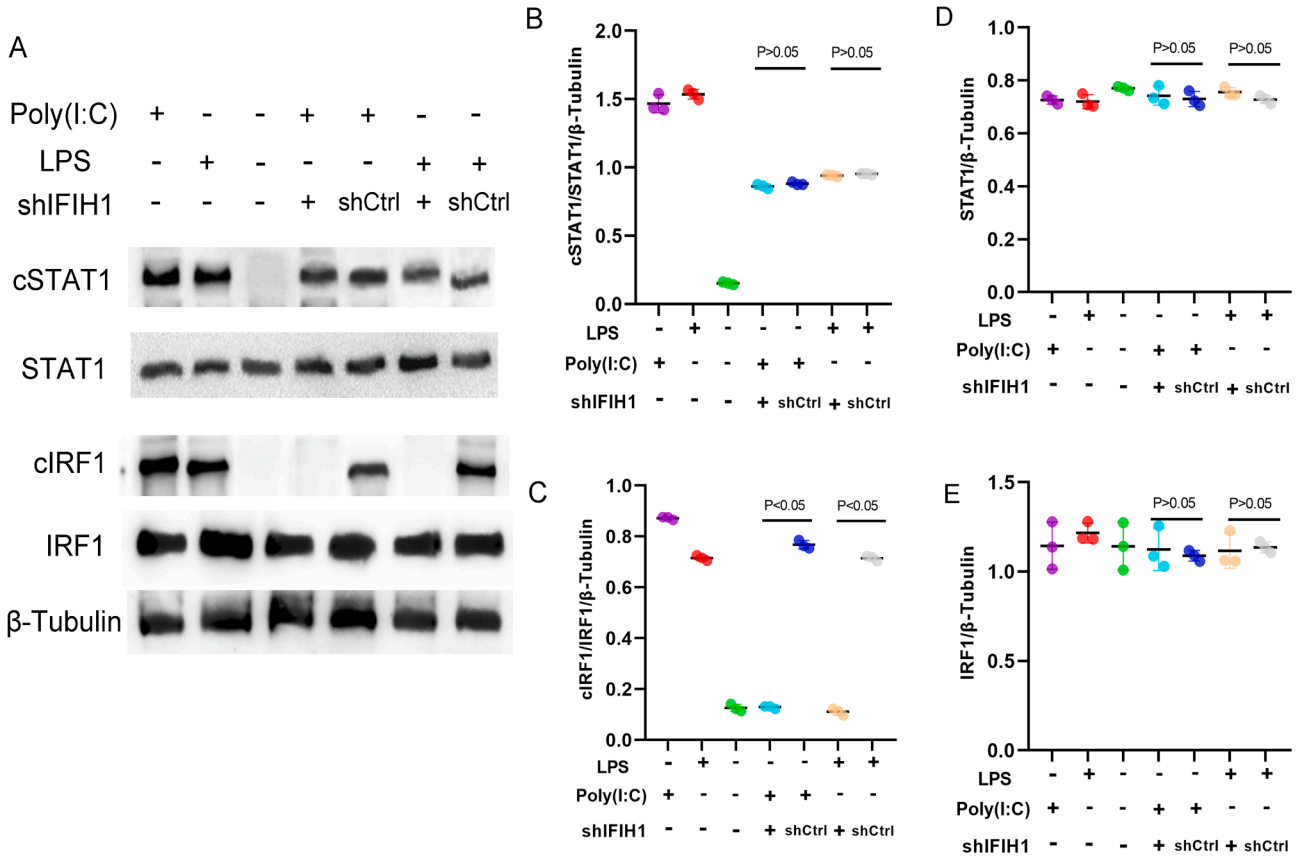

Fig. 4. In response to both Poly(I:C)-induced and LPS-induced circumstances, IFIH1 knockdown inhibited IRF1 translocation into the nucleus. Three mice were included in each group. (A) IRF1 and STAT1 expression in the nucleus as well as total IRF1 and STAT1 levels were examined using Western blotting in each set of BMDMs (n = 3 for each group). (B) IFIH1 knockdown had no effect on STAT1 translocation into the cell nucleus, according to quantitative measurement of STAT1 in the cell nucleus, ($P > 0.05$, n = 3 for each group). (C) Comparing the effects of IFIH1 silencing to the control treatment, quantitative examination of IRF1 in the cell nucleus revealed that both Poly(I:C)-induced and LPS-induced expression of IRF1 in BMDMs nuclei was significantly reduced ($P < 0.05$, n = 3 for each group). (D/E) Compared with the control treatment, IFIH1 knockdown had no effect on STAT1 and IRF1 protein expression in BMDMs ($P < 0.05$, n = 3 for each group). The vector transfection of shIFIH1 and control shRNA had no effect on the expression of IRF1 and STAT1 in BMDMs' nucleus. The statistical analysis was from three independent experiments, and the bar indicates the SD values.

STAT1 compared with the IgG group.

These results indicate that IRF1 is the transcription factor (TF) of STAT1.

Fig. 6 illuminates the molecular mechanism of this study.

4. Discussion

Sepsis-induced ARDS is a lung injury condition caused by dysregulation of the systemic inflammatory host response to infections [25–28]. Macrophage M1 polarization fuels the inflammatory process [29]. We conducted an interrelated bioinformatics analysis and found that IFIH1, IRF1 and STAT1 are all associated with sepsis-induced ARDS as well as macrophage M1polarization.Previous studies have confirmed that IFIH1 and STAT1 regulate macrophage M1 polarization and promote the development of inflammatory diseases, including sepsis-induced ARDS. The current study further indicated that IRF1 contributes to M1-macrophage polarization and the development of sepsis-induced ARDS both in vivo and in vitro. Furthermore, molecular experiments revealed the underlying mechanisms of this link: infection activates IFIH1, which triggers the nuclear translocation of the transcription factor IRF1. IRF1 then attaches to the STAT1 promoter region to initiate the transcription of STAT1 and macrophage M1 polarization.

IFIH1 is a cytosolic receptor responsible for binding viral RNA and activating IFN regulatory factor 3 (IRF3),resulting in the induction of inflammatory and antiviral genes [30–32].Accumulating evidence of the pro-inflammatory function of IFIH1, together with updated studies, suggests that LPS and RNA mimics can both trigger IFIH1 and IRF1 activation. Our previous study and a study by Stone et al. identified IFIH1 as a regulator of macrophage M1 polarization, contributing to the development of sepsis-induced ARDS. Li et al. indicated that IFIH1 mediates the activation and upregulation of STAT1 [32]. Our present study further revealed the underlying mechanism; namely, IFIH1 facilitates the translocation of IRF1, the upstream transcription factor of STAT1, into the nucleus, leading to upregulation of STAT1 expression.

IRF1 is an important antiviral molecule and is implicated in HIV susceptibility and pathogenesis. Specifically, after infection with simian immunodeficiency virus, IFN-(α,β)-producing plasmatoid dendritic cells, macrophages, and large increases in IFN-γ expression were found in cervical vaginal tissues[33]. These findings are especially interesting because IRF1 is a critical TF in the IFN pathway. Zhu et al. and Guo et al. found that miR-19a-3p and miR-130b-3p regulate macrophage M1 polarization through the suppression of the STAT1/IRF1 pathway in the RAW264.7 cell line [23,24]. However, in these studies, the impact of IRF1 on macrophage M1 polarization and ARDS was not convincingly demonstrated within vitro or in vivo experiments, nor were they validated in primary cells (particularly gene knockout mice). The present study included IRF1 deletion, rescue, and over-expression to provide solid evidence that IRF1 is an essential molecule for macrophage M1 polarization, which promotes inflammatory lung damage in CLP-induced sepsis-induced ARDS. ChIP and further experiment indicate that IRF1 is the TF of STAT1 and thus increases STAT1 expression.

TFs that regulate macrophage M1 polarization, such as STAT1, are

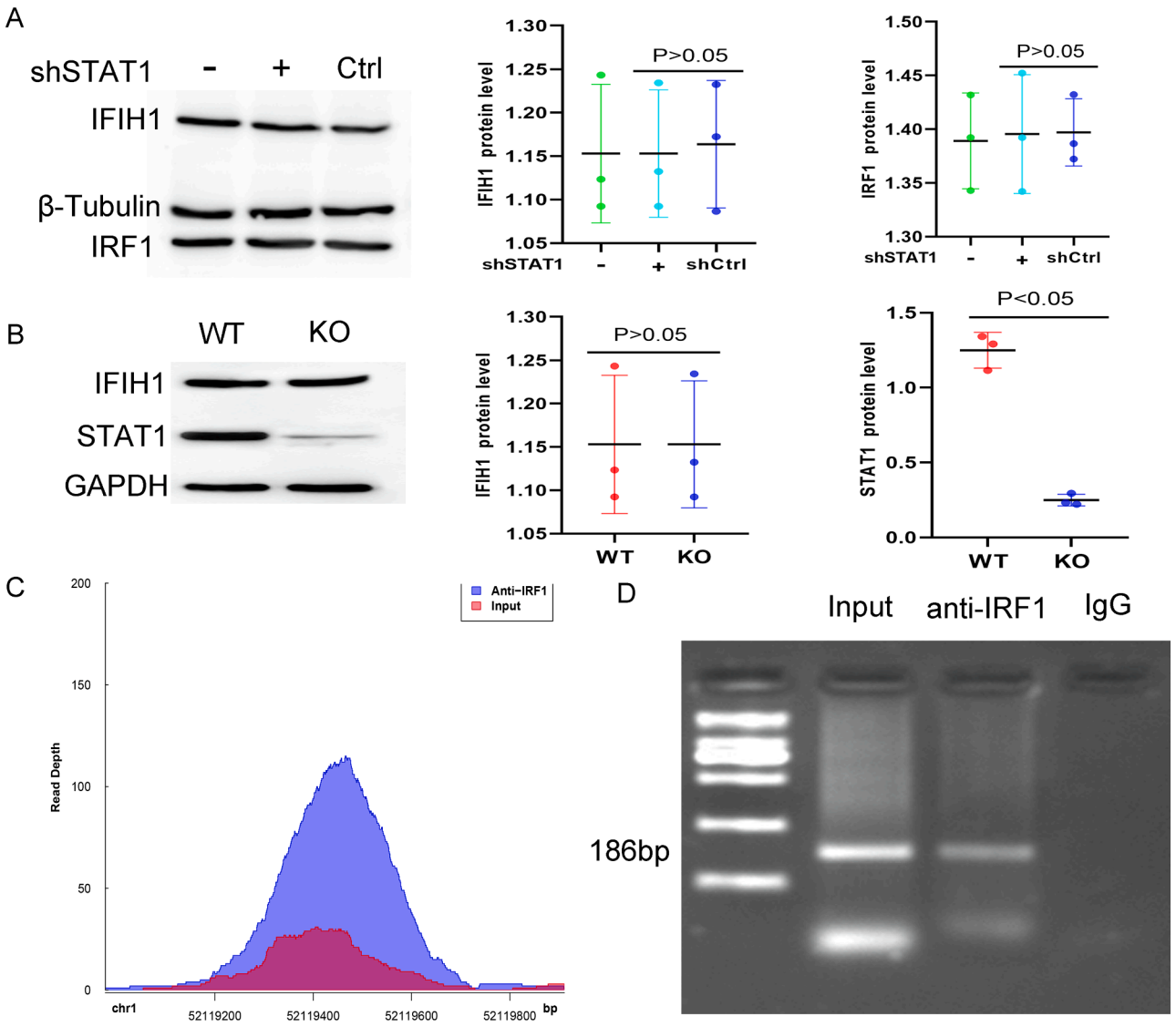

Fig. 5. IRF1 was the transcription factor of STAT1. Three mice were included in each group. (A) Western blotting was performed to detect the expression of IRF1 and IFIH1 after STAT1 knocking down. The results indicated that STAT1 knockdown did not influence the expression of IRF1 and IFIH1 ($P > 0.05$, n = 3 for each group). (B) Western blotting was performed to detect the expression of STAT1 and IFIH1 after IRF1 knocking out. The results indicated that IRF1 knockout markedly decrease STAT1 expression ($P < 0.05$), but did not influence the expression of IFIH1 ($P > 0.05$, n = 3 for each group). (C) CHIP-seq indicated that IRF1 binds to the promoter region of STAT1, compared with input ($FDR < 0.05$, n = 3 for each group). (D) CHIP-PCR further validated that IRF1 to the promoter region of STAT1($P > 0.05$, n = 3 for each group).

robustly expressed in classically activated macrophages and regulate the macrophage inflammatory response [33]. The polarization of macrophages to the M1 phenotype depends on the activation of the TLR4 or IFN-γ pathways, which in turn activate the ERK, NFκB, and STAT1 pathways [34]. Specifically, IFN-α is known to initiate signal transducers and STAT1 signalling, which upregulates the gene expression of interferon regulatory factor-1, a key transcription factor necessary for the cytotoxicity of NK cells, as well as the expression of the effector molecules Fas-L and perforin[35]. Previous studies revealed that IFN-I triggers STAT1 activation. However, the current study indicates that the IFIH1/IRF1 pathway enhances STAT1 upregulation because IRF1 is the TF of STAT1, synergizing with IFN-I-induced STAT1 activation.

5. Conclusion

IRF1 has been identified as the essential molecule that controls the polarization of M1 macrophages and the onset of septic ARDS both in vivo and in vitro. Additionally, IFIH1 promotes IRF1 (transcription factor) translocation into the nucleus to initiate STAT1 transcription as the adapter in response to infection mimic irritants.

Declarations.

Ethics approval and consent to participate

The revised Helsinki Declaration was followed when conducting the current study. The Critical Care Centre at Zhongda Hospital's biological specimen bank provided the samples from the individuals who were included. The Institutional Ethics Committee of Zhongda Hospital approved and oversaw the establishment of this specimen bank in 2017. (number: 2017ZDSYLL105). Figure S1 displayed the Ethical documents.

Animal research in the current study were evaluated and authorized by the Jinan Central Hospital's Animal Care and Use Committee, shown in Figure S2.

Consent for publication.

Not applicable.

Availability of data and materials.

The high-through dataset was down loaded from the GEO public database (GSE46903). Xue J, Schmidt SV, Sander J, Draffehn A, Krebs

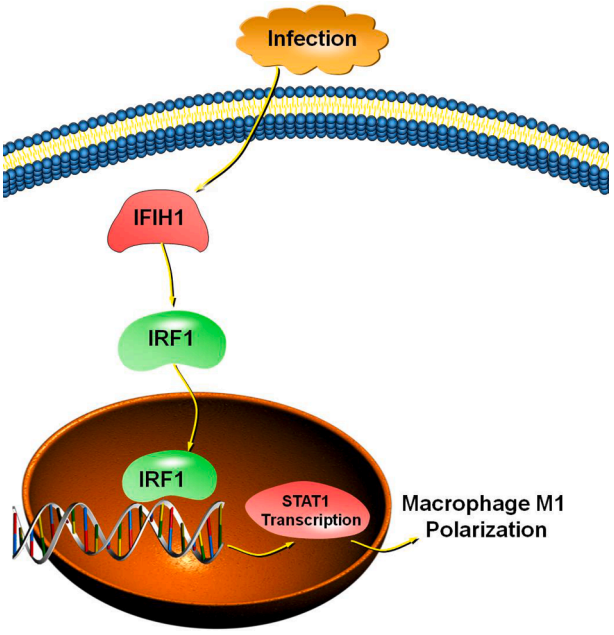

Fig. 6. The molecular mechanism link of IFIH1/IRF1/STAT1 induced macrophage M1 polarization. IFIH1 is activated by infection, which triggers the nuclear translocation of the transcription factor IRF1. IRF1 then attaches to the STAT1 promoter region to initiate the transcription of STAT1 and polarization of macrophage M1.

W, et al. Transcriptome-based network analysis reveals a spectrum model of human macrophage activation.2014. https://www.ncbi.nlm.nih.gov/geo/query/acc.cgi?acc = GSE46903.

Further information and requests for resources and reagents should be directed to and will be fulfilled by the first author, Shi Zhang, E-mail: 394873967@qq.com.

Funding

Supported in part by grants from.

National Natural Science Foundation of China (Grant No: 8220081418);
National Natural Science Foundation of Shandong (Grant No: ZR2022QH332);
Jinan Science and Technology Bureau's Clinical Technology Innovation Program (Grant No: 202134058);
Scientific Research Start-up Funds for talent introduction of Jinan Central hospital (Grant No: YJRC2021010);

Declaration of Competing Interest

The authors declare that they have no known competing financial interests or personal relationships that could have appeared to influence the work reported in this paper.

Data availability

The authors do not have permission to share data.

Acknowledgements

We would like to thank all the editors, reviewers and scholars due to their contribution on this study

Appendix A. Supplementary material

Supplementary data to this article can be found online at https://doi.org/10.1016/j.intimp.2022.109478.

References

[1] G. Bellani, J.G. Laffey, T. Pham, E. Fan, L. Brochard, A. Esteban, et al., Epidemiology, patterns of care, and mortality for patients with acuterespiratory distress syndrome in intensive care units in 50 countries, JAMA 23 (319) (2016 Feb) 698–710.
[2] F. Zhou, T. Yu, R. Du, G. Fan, Y. Liu, Z. Liu, et al., Clinical course and risk factors for mortality of adult inpatients with COVID-19 in Wuhan, China: a retrospective cohort study, Lancet. 395 (10229) (2020 Mar 28) 1054–1062.
[3] L. Liu, Y. Yang, Z. Gao, M. Li, X. Mu, X. Ma, et al., Practice of diagnosis and management of acute respiratory distress syndrome in mainland China: a cross-sectional study, J. Thorac. Dis. 10 (9) (2018 Sep) 5394–5404.
[4] S. Lin, H. Wu, C. Wang, Z. Xiao, F. Xu, Regulatory T Cells and Acute Lung Injury: Cytokines, Uncontrolled Inflammation, and Therapeutic Implications, Front Immunol. 9 (9) (2018 Jul) 1545.
[5] N.J. Meyer, L. Gattinoni, C.S. Calfee, Acute respiratory distress syndrome, Lancet. 398 (10300) (2021 Aug 14) 622–637.
[6] M. Garnier, A. Gibelin, A.A. Mailleux, V. Leçon, M. Hurtado-Nedelec, J. Laschet, et al., Macrophage polarization favors epithelial repair during acute respiratory distress syndrome, Crit. Care Med. 46 (7) (2018 Jul) e692–e701.
[7] S. Zhang, Z. Wu, W. Chang, F. Liu, J. Xie, Y. Yang, H. Qiu, Classification of patients with sepsis according to immune cell characteristics: a bioinformatic analysis of two cohort studies, Front Med (Lausanne). 3 (7) (2020 Dec), 598652.
[8] S. Zhang, C. Chu, Z. Wu, F. Liu, J. Xie, Y. Yang, H. Qiu, IFIH1 Contributes to M1 Macrophage Polarization in ARDS, Front Immunol. 14 (11) (2021 Jan), 580838.
[9] S. Ahmad, X. Mu, F. Yang, E. Greenwald, J.W. Park, E. Jacob, et al., Breaching Self-Tolerance to Alu Duplex RNA Underlies MDA5-Mediated Inflammation, Cell. 172 (4) (2018 Feb 8) 797–810.e13.
[10] A.E.L. Stone, R. Green, C. Wilkins, E.A. Hemann, M. Gale Jr., RIG-I-like receptors direct inflammatory macrophage polarization against West Nile virus infection, Nat. Commun. 10 (1) (2019 Aug 13) 3649.
[11] Gan ZS, Wang QQ, Li JH, Wang XL, Wang YZ, Du HH. Iron Reduces M1 Macrophage Polarization in RAW264.7 Macrophages Associated with Inhibition of STAT1. Mediators Inflamm. 2017;2017:8570818. Epub 2017 Feb 13.
[12] Y. Liu, Z. Liu, H. Tang, Y. Shen, Z. Gong, N. Xie, et al., The N6-methyladenosine (m6A)-forming enzyme METTL3 facilitates M1 macrophage polarization through the methylation of STAT1 mRNA, Am. J. Physiol. Cell Physiol. 317 (4) (2019 Oct 1) C762–C775.
[13] Guo FM, Qiu HB. Definition and dignosis of sepsis 3.0. Zhonghua Nei Ke Za Zhi. 2016 Jun;55(6):420-2.
[14] B.T. Thompson, R.C. Chambers, K.D. Liu, Acute respiratory distress syndrome, N Engl J Med 377 (19) (2017) 1904–1905.
[15] P. Langfelder, S. Horvath, WGCNA: an R package for weighted correlation network analysis, BMC Bioinformatics. 29 (9) (2008 Dec) 559.
[16] J. Xue, S.V. Schmidt, J. Sander, A. Draffehn, W. Krebs, I. Quester, et al., Transcriptome-based network analysis reveals a spectrum model of human macrophage activation, Immunity. 40 (2) (2014 Feb 20) 274–288.
[17] M.D. Robinson, D.J. McCarthy, G.K. Smyth, edgeR: a Bioconductor package for differential expression analysis of digital gene expression data, Bioinformatics. 26 (1) (2010 Jan 1) 139–140.
[18] M.E. Ritchie, B. Phipson, D. Wu, Y. Hu, C.W. Law, W. Shi, et al., limma powers differential expression analyses for RNA-sequencing and microarray studies, Nucleic Acids Res. 43 (7) (2015 Apr 20) e47.
[19] U. Stelzl, U. Worm, M. Lalowski, C. Haenig, F.H. Brembeck, H. Goehler, et al., A human protein-protein interaction network: a resource for annotating the proteome, Cell. 122 (6) (2005 Sep 23) 957–968.
[20] X. Lai, U. Schmitz, S.K. Gupta, A. Bhattacharya, M. Kunz, O. Wolkenhauer, et al., Computational analysis of target hub gene repression regulated by multiple and cooperative miRNAs, Nucleic Acids Res. 40 (18) (2012) 8818–8834.
[21] Z. Cui, Y. Liu, J. Zhang, X. Qiu, Super-delta2: an enhanced differential expression analysis procedure for multi-group comparisons of RNA-seq Data, Bioinformatics. (2021). Mar 8:btab155.
[22] J. Wang, H. Li, B. Xue, R. Deng, X. Huang, Y. Xu, et al., IRF1 Promotes the innate immune response to viral infection by enhancing the activation of IRF3, J Virol. 94 (22) (2020 Oct 27) e01231–e10320.
[23] X. Zhu, Q. Guo, J. Zou, B. Wang, Z. Zhang, R. Wei, et al., MiR-19a-3p Suppresses M1 Macrophage Polarization by Inhibiting STAT1/IRF1 Pathway, Front Pharmacol. 4 (12) (2021 May), 614044.
[24] Q. Guo, X. Zhu, R. Wei, L. Zhao, Z. Zhang, X. Yin, et al., miR-130b-3p regulates M1 macrophage polarization via targeting IRF1, J. Cell Physiol. 236 (3) (2021 Mar) 2008–2022.
[25] F. Liu, J. Xie, X. Zhang, Z. Wu, S. Zhang, M. Xue, et al., Overexpressing TGF-β1 in mesenchymal stem cells attenuates organ dysfunction during CLP-induced septic mice by reducing macrophage-driven inflammation, Stem cell res. therapy 11 (1) (2020) 378.
[26] B. Guillen-Guio, J.M. Lorenzo-Salazar, S.F. Ma, P.C. Hou, T. Hernandez-Beeftink, A. Corrales, et al., Sepsis-associated acute respiratory distress syndrome in individuals of European ancestry: a genome-wide association study, Lancet Respir. Med. 8 (3) (2020 Mar) 258–266.

[27] S. Zhang, W. Chang, J. Xie, Z. Wu, Y. Yang, H. Qiu, The efficacy, safety, and optimal regimen of corticosteroids in sepsis: a bayesian network meta-analysis, Crit. Care Explor. 2 (4) (2020 Apr 29) e0094.
[28] S. Zhang, F. Liu, Z. Wu, J. Xie, Y. Yang, H. Qiu, Contribution of m6A subtype classification on heterogeneity of sepsis, Ann Transl Med. 8 (6) (2020 Mar) 306.
[29] Y. Jiao, T. Zhang, C. Zhang, H. Ji, X. Tong, R. Xia, et al., Exosomal miR-30d-5p of neutrophils induces M1 macrophage polarization and primes macrophage pyroptosis in sepsis-related acute lung injury, Crit. Care. 25 (1) (2021 Oct 12) 356.
[30] W. Lee, S.H. Lee, M. Kim, J.S. Moon, G.W. Kim, H.G. Jung, et al., Vibrio vulnificus quorum-sensing molecule cyclo (Phe-Pro) inhibits RIG-I-mediated antiviral innate immunity, Nat. Commun. 9 (2018) 1606.
[31] Jaeger M, van der Lee R, Cheng SC, Johnson MD, Kumar V, Ng A, et al. The RIG-I-like helicase receptor MDA5 (IFIH1) is involved in the host defense against Candida infections. Eur J Clin Microbiol Infect Dis (2015) 2015-05-0134(5):963–74.
[32] Y. Li, P. Yu, C. Qu, P. Li, Y. Li, Z. Ma, et al., MDA5 against enteric viruses through induction of interferon-like response partially via the JAK-STAT cascade, Antiviral Res. 176 (2020 Apr), 104743, https://doi.org/10.1016/j.antiviral.2020.104743. Epub 2020 Feb 10 PMID: 32057771.
[33] S. Roy, S. Schmeier, E. Arner, T. Alam, S.P. Parihar, M. Ozturk, et al., Redefining the transcriptional regulatory dynamics of classically and alternatively activated macrophages by deep CAGE transcriptomics, Nucleic Acids Res. 43 (14) (2015 Aug 18) 6969–6982.
[34] G. Ma, P.Y. Pan, S. Eisenstein, C.M. Divino, C.A. Lowell, T. Takai, et al., Paired immunoglobin-like receptor-B regulates the suppressive function and fate of myeloid-derived suppressor cells, Immunity. 34 (3) (2011 Mar 25) 385–395.
[35] Ahlenstiel G, Titerence RH, Koh C, Edlich B, Feld JJ, Rotman Y, et al. Natural killer cells are polarized toward cytotoxicity in chronic hepatitis C in an interferon-alfa-dependent manner. Gastroenterology. 2010 Jan;138(1):325-35.e1-2.